

KIAS-P99110  
hep-ph/9912330  
December 1999

# Probing MSSM Higgs Sector with Explicit CP Violation at a Photon Linear Collider

S.Y. Choi and Jae Sik Lee  
*Korea Institute for Advanced Study, Seoul 130-012, Korea*

## Abstract

The  $CP$  properties of Higgs bosons can be probed through their  $s$ -channel resonance productions via photon–photon collisions by use of circularly and/or linearly polarized backscattered laser photons at a TeV-scale linear  $e^+e^-$  collider. Exploiting this powerful tool, we investigate in detail the Higgs sector of the minimal supersymmetric Standard Model with explicit  $CP$  violation.

PACS number(s): 11.30.Er, 12.60.Jv, 13.10.+q

## I. INTRODUCTION

The minimal supersymmetric standard model (MSSM), of which the Higgs sector is a well-defined two-Higgs-doublet model (2HDM), contains several  $CP$ -violating phases absent in the Standard Model (SM). In particular, the  $CP$ -violating phases of the higgsino mass parameter  $\mu$  and of the stop and sbottom trilinear couplings  $A_t$  and  $A_b$  can affect the neutral Higgs sector significantly at the loop level due to the large Yukawa couplings, leading to a large mixing between the  $CP$ -even and  $CP$ -odd neutral Higgs bosons as well as to an induced relative phase  $\xi$  between the vacuum expectation values of the two Higgs doublets [1,2].

The  $CP$ -violating phases do not have to be suppressed in order to satisfy the present experimental constraints from the electron and neutron electric dipole moments (EDMs) [3]. This has been shown, for example, in the context of the so-called effective supersymmetry (SUSY) model [4] where the first and second generation sfermions are decoupled, but the third generation sfermions remain relatively light to preserve naturalness. Based on the scenarios of this type, the sensitivities of a variety of experimental observables to  $CP$  violation in the sfermion sector as well as the neutral Higgs sector have been recently examined in  $B$  decays [5], supersymmetric dark-matter searches, and production of sparticles and Higgs bosons at LEP II, LHC and muon colliders [1,6,7].

One of the cleanest determinations of the neutral Higgs sector  $CP$  violation in the MSSM can be achieved by observing the  $CP$  properties of all three neutral Higgs particles directly. In this light, the  $s$ -channel resonance production of neutral Higgs bosons in  $\gamma\gamma$  collisions [8] has long been recognized as an important instrument to study the  $CP$  properties of Higgs particles [9,10] at a linear  $e^+e^-$  collider (LC) by use of polarized high energy laser lights obtained by Compton back-scattering of polarized laser light off the electron and positron beams [11]. In the context of a general 2HDM involving a lot of free parameters, the powerfulness of the production mechanism has been demonstrated by Grzadkowski and Gunion [9]. On the contrary, the parameters determining the MSSM Higgs sector  $CP$  violation are well defined so that the dependence of the  $CP$  violation in the Higgs sector on the relevant parameters can be explicitly studied. So, in this paper, we demonstrate that polarized back-scattered laser photons at a TeV-scale LC enable us to investigate the  $CP$  violation of the Higgs sector in the MSSM through  $s$ -channel Higgs-boson production via  $\gamma\gamma$  collisions in detail including its dependence on the relevant SUSY parameters.

In Sec. II we briefly review the  $CP$ -violating Higgs-boson mixing in the MSSM induced at the loop-level from the stop and sbottom sectors due to the complex higgsino mass parameter,  $\mu$ , and trilinear couplings,  $A_t$  and  $A_b$ . Sec. III is devoted to a model-independent description of the  $s$ -channel Higgs-boson production in polarized  $\gamma\gamma$  collisions leading to three polarization asymmetries expressed in terms of two complex form factors for each neutral Higgs boson; one form factor is  $CP$ -even and the other one  $CP$ -odd. Then we briefly describe the mechanism of generating polarized back-scattered laser photons and controlling the polarizations of the generated photons at a LC. In Sec. IV, we present the analytic form of the  $CP$ -even and  $CP$ -odd form factors explicitly in terms of the relevant SUSY parameters in the MSSM with explicit  $CP$  violation. And in Sec. V we investigate in detail the dependence of the total production rates and the three polarization asymmetries on the  $CP$ -violating phases with the values of the other SUSY parameters fixed. The conclusion

is given in Sec. VI and all the interaction Lagrangian terms needed for the present work are listed in the Appendix.

## II. CP–VIOLATING NEUTRAL HIGGS–BOSON MIXING

The most general  $CP$ –violating Higgs potential of the MSSM can conveniently be described by the effective Lagrangian [2]:

$$\begin{aligned}\mathcal{L}_V = & \mu_1^2(\Phi_1^\dagger\Phi_1) + \mu_1^2(\Phi_2^\dagger\Phi_2) + m_{12}^2(\Phi_1^\dagger\Phi_2) + m_{12}^{*2}(\Phi_2^\dagger\Phi_1) \\ & + \lambda_1(\Phi_1^\dagger\Phi_1)^2 + \lambda_2(\Phi_2^\dagger\Phi_2)^2 + \lambda_3(\Phi_1^\dagger\Phi_1)(\Phi_2^\dagger\Phi_2) + \lambda_4(\Phi_1^\dagger\Phi_2)(\Phi_2^\dagger\Phi_1) \\ & + \lambda_5(\Phi_1^\dagger\Phi_2)^2 + \lambda_5^*(\Phi_2^\dagger\Phi_1)^2 + \lambda_6(\Phi_1^\dagger\Phi_1)(\Phi_1^\dagger\Phi_2) + \lambda_6^*(\Phi_1^\dagger\Phi_1)(\Phi_2^\dagger\Phi_1) \\ & + \lambda_7(\Phi_2^\dagger\Phi_2)(\Phi_1^\dagger\Phi_2) + \lambda_7^*(\Phi_2^\dagger\Phi_2)(\Phi_2^\dagger\Phi_1),\end{aligned}\quad (1)$$

where for convenience  $\Phi_1 = +i\tau_2 H_1^*$  and  $\Phi_2 = H_2$  are introduced instead of the conventional MSSM Higgs doublets  $H_1$  and  $H_2$ . At the tree level,  $\mu_1^2 = -m_1^2 - |\mu|^2$  and  $\mu_2^2 = -m_2^2 - |\mu|^2$  with  $m_1^2$ ,  $m_2^2$ , and  $m_{12}^2$  the soft–SUSY–breaking parameters related to the Higgs sector, and the first four quartic couplings are determined solely by the SM gauge couplings;  $\lambda_1 = \lambda_2 = -\frac{1}{8}(g^2 + g'^2)$ ,  $\lambda_3 = -\frac{1}{4}(g^2 - g'^2)$ , and  $\lambda_4 = \frac{1}{2}g^2$ , while the remaining three quartic couplings vanish;  $\lambda_5 = \lambda_6 = \lambda_7 = 0$ . Beyond the Born approximation, however, the quartic couplings  $\{\lambda_5, \lambda_6, \lambda_7\}$  can receive significant radiative corrections due to large Yukawa couplings of the Higgs fields to the top/bottom and stop/sbottom sectors. The analytic expressions of these parameters, which are in general complex, can be found in the Appendix of Ref. [2].

The  $CP$ –violating radiatively–corrected quartic couplings cause three physical neutral Higgs bosons to mix with one another. In order to describe the  $CP$ –violating Higgs–boson mixing, it is first of all necessary to determine the ground state of the Higgs potential. To this end we introduce the linear decompositions of the Higgs fields

$$\Phi_1 = \begin{pmatrix} \phi_1^+ \\ \frac{1}{\sqrt{2}}(v_1 + \phi_1 + ia_1) \end{pmatrix}, \quad \Phi_2 = e^{i\xi} \begin{pmatrix} \phi_2^+ \\ \frac{1}{\sqrt{2}}(v_2 + \phi_2 + ia_2) \end{pmatrix}, \quad (2)$$

with  $v_1$  and  $v_2$  the moduli of the vacuum expectation values (VEVs) of the Higgs doublets and  $\xi$  is their relative phase. These VEVs and the relative phase can be determined by the minimization conditions on  $\mathcal{L}_V$ . It is always guaranteed that one combination of the  $CP$ –odd Higgs fields  $a_1$  and  $a_2$  ( $G^0 = \cos\beta a_1 + \sin\beta a_2$ ) defines a flat direction in the Higgs potential and it is absorbed as the longitudinal component of the  $Z$  field. Denoting the remaining  $CP$ –odd state  $a = -\sin\beta a_1 + \cos\beta a_2$ , the neutral Higgs–boson mass matrix describing the mixing between  $CP$ –even and  $CP$ –odd fields in the  $(a, \phi_1, \phi_2)$  basis is given by

$$\mathcal{M}_N^2 = \begin{pmatrix} \mathcal{M}_P^2 & (\mathcal{M}_{SP}^2)^T \\ \mathcal{M}_{SP}^2 & \mathcal{M}_S^2 \end{pmatrix}. \quad (3)$$

The analytic form of the sub-matrices is given by

$$\mathcal{M}_P^2 = m_a^2 = \frac{1}{s_\beta c_\beta} \left\{ \mathcal{R}(m_{12}^2 e^{i\xi}) + v^2 \left[ 2\mathcal{R}(\lambda_5 e^{2i\xi}) s_\beta c_\beta + \frac{1}{2}\mathcal{R}(\lambda_6 e^{i\xi}) c_\beta^2 + \frac{1}{2}\mathcal{R}(\lambda_7 e^{i\xi}) s_\beta^2 \right] \right\},$$

$$\begin{aligned}
\mathcal{M}_{SP}^2 &= v^2 \begin{pmatrix} \mathcal{I}(\lambda_5 e^{2i\xi}) s_\beta + \mathcal{I}(\lambda_6 e^{i\xi}) c_\beta \\ \mathcal{I}(\lambda_5 e^{2i\xi}) c_\beta + \mathcal{I}(\lambda_7 e^{i\xi}) s_\beta \end{pmatrix}, \\
\mathcal{M}_S^2 &= m_a^2 \begin{pmatrix} s_\beta^2 & -s_\beta c_\beta \\ -s_\beta c_\beta & c_\beta^2 \end{pmatrix} \\
&- v^2 \begin{pmatrix} 2\lambda_1 c_\beta^2 + 2\mathcal{R}(\lambda_5 e^{2i\xi}) s_\beta^2 + 2\mathcal{R}(\lambda_6 e^{i\xi}) s_\beta c_\beta & \lambda_{34} s_\beta c_\beta + \mathcal{R}(\lambda_6 e^{i\xi}) c_\beta^2 + \mathcal{R}(\lambda_7 e^{i\xi}) s_\beta^2 \\ \lambda_{34} s_\beta c_\beta + \mathcal{R}(\lambda_6 e^{i\xi}) c_\beta^2 + \mathcal{R}(\lambda_7 e^{i\xi}) s_\beta^2 & 2\lambda_2 s_\beta^2 + 2\mathcal{R}(\lambda_5 e^{2i\xi}) c_\beta^2 + 2\mathcal{R}(\lambda_7 e^{i\xi}) s_\beta c_\beta \end{pmatrix}. \quad (4)
\end{aligned}$$

The  $CP$ –even and  $CP$ –odd Higgs–boson states mix unless all the imaginary parts of the parameters  $\lambda_5, \lambda_6, \lambda_7$  vanish<sup>1</sup> and the symmetric Higgs–boson mass matrix  $\mathcal{M}_N^2$  can be diagonalized by a  $3 \times 3$  orthogonal matrix  $O$  relating the weak eigenstates to the mass eigenstates as

$$(a, \phi_1, \phi_2)^T = O (H_3, H_2, H_1)^T, \quad (5)$$

with the mass ordering of  $m_{H_1} \leq m_{H_2} \leq m_{H_3}$ .

The characteristic size of the  $CP$ –violating neutral Higgs–boson mixing is determined by the factor

$$\frac{1}{32\pi^2} \frac{Y_f^4 |\mu| |A_f|}{M_{\text{SUSY}}^2} \sin \Phi_{A_f \mu}, \quad (6)$$

where  $Y_f$  is the Yukawa coupling of the fermion  $f$ ,  $\Phi_{A_f \mu} = \text{Arg}(A_f \mu) + \xi$  for  $f = t, b$ , and  $M_{\text{SUSY}}$  is a typical SUSY–breaking scale, of which the square might be taken to be the average of the two sfermion masses squared, i.e.  $M_{\text{SUSY}}^2 = (m_{\tilde{f}_1}^2 + m_{\tilde{f}_2}^2)/2$ . The neutral Higgs–boson mixing modifies not only the Higgs mass spectra but also their couplings to fermions, to sfermions, to the  $W$  and  $Z$  gauge bosons, and to the Higgs bosons themselves significantly. (See the Appendix to find the interaction Lagrangian terms for the couplings of the Higgs bosons with the fermions and bosons). Therefore, the  $CP$ –violating mixing can affect the cross section of the process  $\gamma\gamma \rightarrow H_i$  ( $i = 1, 2, 3$ ) significantly because the two–photon fusion process is mediated by loops of all charged particles with non–zero mass.

Although the stop and sbottom trilinear parameters are in general independent, we assume for our numerical analysis a universal trilinear parameter  $A \equiv A_t = A_b$  and we vary the phase  $\Phi = \Phi_\mu + \Phi_A$ , where  $\Phi_A$  is the phase of the universal parameter  $A$ , over the range  $[0^\circ, 360^\circ]$  and the charged Higgs–boson mass  $m_{H^\pm}$  up to 1 TeV. In addition, noting that the  $CP$ –violating phases could weaken the present experimental bounds on the lightest Higgs mass up to about 60 GeV [2], we simply apply the lower mass limit  $M_{H_1} \geq 70$  GeV to the lightest Higgs–boson determining the lowest allowed value of  $M_{H^\pm}$  for a given set of SUSY parameters. For the parameter  $\tan \beta$ , we take  $\tan \beta = 3$  or 10 as the values representing the small and large  $\tan \beta$  cases, respectively. Finally, we take for the remaining dimensionful parameters

$$|A| = 0.4 \text{ TeV}, \quad |\mu| = 1.2 \text{ TeV}, \quad M_{\text{SUSY}} = 0.5 \text{ TeV}, \quad \Delta_t = \Delta_b = M_{\text{SUSY}}^2, \quad (7)$$

---

<sup>1</sup> If all the imaginary parts of  $\lambda_i$  ( $i = 5, 6, 7$ ) are zero, the induced phase  $\xi$  vanish as well.

with  $\Delta_f = m_{\tilde{f}_2}^2 - m_{\tilde{f}_1}^2$  for  $f = t, b$ , safely avoiding the two-loop EDM constraints [12]. The parameter set (7) gives a rather large  $CP$ -violating neutral Higgs–boson mixing as can be seen in Eq. (6). However, the dependence of our results on a different parameter set can be easily worked out.

### III. TWO-PHOTON FUSION INTO HIGGS BOSONS

#### A. Model independent description

In the presence of the  $CP$ -violating neutral Higgs–boson mixing, the production amplitude of the two-photon fusion process  $\gamma\gamma \rightarrow H_i$  ( $i = 1, 2, 3$ ) can be parameterized in a model-independent way in terms of two (complex) form factors  $A_i$  and  $B_i$  as

$$\mathcal{M}(\gamma\gamma \rightarrow H_i) = M_{H_i} \frac{\alpha}{4\pi} \left\{ A_i(s) \left[ \epsilon_1 \cdot \epsilon_2 - \frac{2}{s} (\epsilon_1 \cdot k_2)(\epsilon_2 \cdot k_1) \right] - B_i(s) \frac{2}{s} \langle \epsilon_1 \epsilon_2 k_1 k_2 \rangle \right\}, \quad (8)$$

where  $s$  is the c.m. energy squared of two colliding photons and the notation  $\langle \epsilon_1 \epsilon_2 k_1 k_2 \rangle$  stands for the Lorentz invariant contraction  $\epsilon_{\mu\nu\alpha\beta} \epsilon_1^\mu \epsilon_2^\nu k_1^\alpha k_2^\beta$ . In the two-photon c.m coordinate system with one photon momentum  $\vec{k}_1$  along the positive  $z$  direction and the other one  $\vec{k}_2$  along the negative  $z$  direction, the wave vectors  $\epsilon_{1,2}$  of two photons are given by

$$\epsilon_1(\lambda) = \epsilon_2^*(\lambda) = \frac{1}{\sqrt{2}} (0, -\lambda, -i, 0). \quad (9)$$

where  $\lambda = \pm 1$  denote the right and left photon helicities, respectively. Inserting the wave vectors into Eq. (8) we obtain the production helicity amplitude for the photon fusion process as follows

$$\mathcal{M}_{\lambda_1 \lambda_2} = -M_{H_i} \frac{\alpha}{4\pi} \{ A_i(s) \delta_{\lambda_1 \lambda_2} + i \lambda_1 B_i(s) \delta_{\lambda_1 \lambda_2} \}, \quad (10)$$

with  $\lambda_{1,2} = \pm$ , yielding the absolute polarized amplitude squared

$$\overline{|\mathcal{M}|^2} = \overline{|\mathcal{M}|_0^2} \left\{ [1 + \zeta_2 \tilde{\zeta}_2] + \mathcal{A}_1 [\zeta_2 + \tilde{\zeta}_2] + \mathcal{A}_2 [\zeta_1 \tilde{\zeta}_3 + \zeta_3 \tilde{\zeta}_1] - \mathcal{A}_3 [\zeta_1 \tilde{\zeta}_1 - \zeta_3 \tilde{\zeta}_3] \right\}, \quad (11)$$

with the Stokes parameters  $\{\zeta_i\}$  and  $\{\tilde{\zeta}_i\}$  ( $i = 1, 2, 3$ ) of two photon beams, respectively. The first factor in Eq. (11) is the unpolarized amplitude squared;

$$\overline{|\mathcal{M}|_0^2} = \frac{1}{4} \{ |\mathcal{M}_{++}|^2 + |\mathcal{M}_{--}|^2 \}. \quad (12)$$

and three polarization asymmetries  $\mathcal{A}_i$  ( $i = 1, 2, 3$ ) are defined in terms of the helicity amplitudes and expressed in terms of the form factors  $A_i$  and  $B_i$  as

$$\begin{aligned} \mathcal{A}_1 &= \frac{|\mathcal{M}_{++}|^2 - |\mathcal{M}_{--}|^2}{|\mathcal{M}_{++}|^2 + |\mathcal{M}_{--}|^2} = \frac{2\mathcal{I}(A(s)B(s)^*)}{|A(s)|^2 + |B(s)|^2}, \\ \mathcal{A}_2 &= \frac{2\mathcal{I}(\mathcal{M}_{--}^* \mathcal{M}_{++})}{|\mathcal{M}_{++}|^2 + |\mathcal{M}_{--}|^2} = \frac{2\mathcal{R}(A(s)B(s)^*)}{|A(s)|^2 + |B(s)|^2}, \\ \mathcal{A}_3 &= \frac{2\mathcal{R}(\mathcal{M}_{--}^* \mathcal{M}_{++})}{|\mathcal{M}_{++}|^2 + |\mathcal{M}_{--}|^2} = \frac{|A(s)|^2 - |B(s)|^2}{|A(s)|^2 + |B(s)|^2}. \end{aligned} \quad (13)$$

In the  $CP$ -invariant theories with real couplings, the form factors  $A_i$  and  $B_i$  cannot be simultaneously non-vanishing so that they should satisfy the relations;  $\mathcal{A}_1 = \mathcal{A}_2 = 0$  and  $\mathcal{A}_3 = +1(-1)$  depending on whether the Higgs boson is a pure  $CP$ -even ( $CP$ -odd) state. In other words,  $\mathcal{A}_1 \neq 0$ ,  $\mathcal{A}_2 \neq 0$  and/or  $|\mathcal{A}_3| < 1$  ensure a simultaneous existence of non-zero  $A_i$  and  $B_i$  implying  $CP$  violation. Note that the asymmetry  $\mathcal{A}_1$  is non-vanishing only when  $A_i$  and  $B_i$  have a finite relative phase. As will be seen explicitly in the next section, even for the real MSSM couplings  $A_i(s)$  and  $B_i(s)$  could be complex because of the nontrivial developments of the imaginary parts for the Higgs masses larger than twice the loop masses.

In the narrow-width approximation, the partonic cross section of the  $s$ -channel Higgs-boson production  $\gamma\gamma \rightarrow H_i$  can be expressed as

$$\sigma(\gamma\gamma \rightarrow H_i) = \frac{\pi}{M_{H_i}^4} \overline{|\mathcal{M}|_0^2} \delta\left(1 - \frac{M_{H_i}^2}{s}\right) \equiv \hat{\sigma}_0(H_i) \delta\left(1 - \frac{M_{H_i}^2}{s}\right), \quad (14)$$

which is eventually to be folded with a realistic photon luminosity spectrum. Certainly, it is recommended to use as hard photon spectra as possible and to have the capability of controlling photon polarizations with ease. Such a high energy polarized photon beam is available using Compton backscattering of laser light off the electron or positron beams. Although the detailed description of the generation mechanism has been provided in literature, we will describe for our purpose the mechanism briefly in the following subsection.

## B. Polarized high energy laser back-scattered photons

High energy colliding beams of polarized photons can be generated by Compton backscattering of polarized laser light on (polarized) electron/positron bunches of  $e^+e^-$  linear colliders<sup>2</sup>. The polarization transfer from the laser light to the high energy photons is described by three Stokes parameters  $\zeta_{1,2,3}$ ;  $\zeta_2$  is the degree of circular polarization and  $\{\zeta_3, \zeta_1\}$  the degree of linear polarization transverse and normal to the plane defined by the electron direction and the direction of the maximal linear polarization of the initial laser light. Explicitly, the Stokes parameters take the form [11]:

$$\zeta_1 = \frac{f_3(y)}{f_0(y)} P_t \sin 2\kappa, \quad \zeta_2 = -\frac{f_2(y)}{f_0(y)} P_c, \quad \zeta_3 = \frac{f_3(y)}{f_0(y)} P_t \cos 2\kappa, \quad (15)$$

where  $y$  is the energy fraction of the back-scattered photon with respect to the initial electron energy  $E_e$ ,  $\{P_c, P_t\}$  are the degrees of circular and transverse polarization of the initial laser light, and  $\kappa$  is the azimuthal angle between the directions of initial photon and its maximum linear polarization. Similar relations can be obtained for the Stokes parameters  $\tilde{\zeta}$  of the opposite high energy photons by replacing  $(P_c, P_t, \kappa)$  with  $(\tilde{P}_c, \tilde{P}_t, -\tilde{\kappa})$ . The functions  $f_0$ ,  $f_2$ , and  $f_3$  determining the photon energy spectrum and the Stokes parameters are given by

---

<sup>2</sup>In the present work the electron and positron beams are assumed to be unpolarized. It is however straightforward to take into account polarized electron and positron beams.

$$f_0(y) = \frac{1}{1-y} + 1 - y - 4r(1-r), \quad f_2(y) = (2r-1) \left( \frac{1}{1-y} + 1 - y \right), \quad f_3(y) = 2r^2, \quad (16)$$

with  $r = y/x(1-y)$  and  $x = 4E_e\omega_0/m_e^2 \approx 15.4(E_e[\text{TeV}])(\omega_0[\text{eV}])$  for the initial laser energy  $\omega_0$ . We observe in Eqs. (11) and (15) that the linear polarization of the high energy photon beam is proportional to  $P_t$  whereas the circular polarization is proportional to  $P_c$ . Therefore, it is necessary to have both circularly and linearly polarized photons in order to measure all the polarization asymmetries  $\mathcal{A}_{1,2,3}$  and as a result the complex form factors  $A_i(s)$  and  $B_i(s)$ .

After folding the luminosity spectra of two photon beams, the event rate of the Higgs boson production via two-photon fusion is given by

$$\begin{aligned} \frac{dN}{d\eta} = \frac{dL_{\gamma\gamma}}{d\eta} \frac{M_{H_i}^4}{\pi} \hat{\sigma}_0 & \left\{ 1 + P_c \tilde{P}_c \frac{\langle f_2 * f_2 \rangle_\eta}{\langle f_0 * f_0 \rangle_\eta} - \mathcal{A}_1 (P_c + \tilde{P}_c) \frac{\langle f_0 * f_2 \rangle_\eta}{\langle f_0 * f_0 \rangle_\eta} \right. \\ & \left. + P_t \tilde{P}_t [\mathcal{A}_2 \sin 2(\kappa - \tilde{\kappa}) + \mathcal{A}_3 \cos 2(\kappa - \tilde{\kappa})] \frac{\langle f_3 * f_3 \rangle_\eta}{\langle f_0 * f_0 \rangle_\eta} \right\}, \end{aligned} \quad (17)$$

where  $\frac{dL_{\gamma\gamma}}{d\eta}$  is the two-photon luminosity function depending on the details such as the  $e-\gamma$  conversion factor and the shape of the electron/positron bunches [11], and  $\eta \equiv s/s_{ee} = m_{H_i}^2/s_{ee}$ . The luminosity correlation functions  $\langle f_i * f_j \rangle_\eta$  are defined as

$$\langle f_i * f_j \rangle_\eta = \frac{1}{N^2} \int_{\eta/y_{\max}}^{y_{\max}} \frac{dy}{y} f_i(y) f_j(\eta/y), \quad (18)$$

with the normalization  $N = \int_0^{y_{\max}} dy f_0(y)$  and  $y_{\max} = x/(1+x)$ .

We show in Fig. 1 the correlation function  $\langle f_0 * f_0 \rangle_\eta$  and the three ratios of the correlation functions appearing in Eq. (17) for  $x = 0.5$  (solid line), 1.0 (dashed line), and 4.83 (dotted line). For a larger value of  $x$ , the correlation function  $\langle f_0 * f_0 \rangle_\eta$ , to which  $dL_{\gamma\gamma}/d\eta$  is proportional, becomes more flat and the maximal obtainable photon energy fraction becomes closer to the electron beam energy. Exploiting this feature appropriately could facilitate Higgs-boson searches at a photon linear collider. The three figures for the ratios of correlation functions clearly show that the maximal sensitivity to each polarization asymmetry  $\mathcal{A}_i$  can be acquired near the the maximal value of  $\eta = y_{\max}^2$ . Therefore, once the Higgs-boson masses are known, one can obtain the maximal sensitivities by tuning the initial electron energy to be

$$E_e = \left( \frac{1+x}{2x} \right) M_{H_i}. \quad (19)$$

On the other hand, the ratio  $\langle f_3 * f_3 \rangle_\eta / \langle f_0 * f_0 \rangle_\eta$  is larger for a smaller value of  $x$  and for a given  $x$  the maximum value of the ratio is given by

$$\left( \frac{\langle f_3 * f_3 \rangle_\eta}{\langle f_0 * f_0 \rangle_\eta} \right)_{\max} = \left[ \frac{2(1+x)}{1+(1+x)^2} \right]^2. \quad (20)$$

Consequently, it is necessary to take a small  $x$  and a high  $E_e$  by changing the laser beam energy  $\omega_0$  so as to acquire the highest sensitivity to  $CP$  violation in the neutral Higgs sector.

## IV. THE MSSM WITH EXPLICIT CP VIOLATION

In this section, we consider the MSSM as a specific 2HDM, in which the Higgs sector  $CP$  violation is induced at the loop level from the stop and sbottom sectors defined by the trilinear parameters  $A_{t,b}$  and the higgsino mass parameter  $\mu$  [2]. Then, we derive the explicit form of the form factors  $A_i(s)$  and  $B_i(s)$  by calculating the loop contributions from the bottom and top quarks, the charged Higgs boson, the  $W$  boson as well as the lighter top and bottom squarks<sup>3</sup>.

Taking the sum of all the charged particle contributions, we obtain for the form factor  $A_i$  at  $s = M_{H_i}^2$ :

$$A_i(s = M_{H_i}^2) = \sum_{f=t,b} A_i^f + \sum_{\tilde{f}_j = \tilde{t}_1, \tilde{b}_1} A_i^{\tilde{f}_j} + A_i^{H^\pm} + A_i^{W^\pm}, \quad (21)$$

with the  $CP$ -even functions

$$\begin{aligned} A_i^f &= -2 \left( \sqrt{2} G_F \right)^{1/2} M_{H_i} N_c e_f^2 \left( \frac{v_f^i}{R_\beta^f} \right) F_{sf}(\tau_{if}), \\ A_i^{\tilde{f}_j} &= \frac{M_{H_i} N_c e_f^2 g_{\tilde{f}_j \tilde{f}_j}^i}{2 m_{\tilde{f}_j}^2} F_0(\tau_{i\tilde{f}}), \\ A_i^{H^\pm} &= \frac{M_{H_i} v C_i}{2 m_{H^\pm}^2} F_0(\tau_{iH}), \\ A_i^{W^\pm} &= \left( \sqrt{2} G_F \right)^{1/2} M_{H_i} (c_\beta O_{2,4-i} + s_\beta O_{3,4-i}) F_1(\tau_{iW}), \end{aligned} \quad (22)$$

where  $N_c = 3$ , the scaling variable  $\tau_{ix} = m_{H_i}^2 / 4 m_x^2$  for  $m_x = m_f, m_{\tilde{f}_i}, M_{H^\pm}, m_{W^\pm}$ , and the definition of all the *real* couplings  $v_f^i$ ,  $g_{t_1 \tilde{t}_1}^i$ ,  $g_{b_1 \tilde{b}_1}^i$ ,  $C_i$ , and  $O_{\alpha,4-i}$  as well as  $R_\beta^f$  is given in the Appendix. On the other hand, the form factor  $B_i$  related to the fermionic triangle anomaly has the contributions only from the top and bottom quarks and it takes the form

$$B_i(s = M_{H_i}^2) = -2 \left( \sqrt{2} G_F \right)^{1/2} M_{H_i} N_c \sum_{f=t,b} e_f^2 \left( \frac{\bar{R}_\beta^f a_f^i}{R_\beta^f} \right) F_{pf}(\tau_{if}), \quad (23)$$

where the definition of the real couplings  $a_f^i$  also can be found in the Appendix. The form factors  $F_{sf}$ ,  $F_{pf}$ ,  $F_0$ , and  $F_1$  can be expressed as

$$\begin{aligned} F_{sf}(\tau) &= \tau^{-1} [1 + (1 - \tau^{-1}) f(\tau)], & F_{pf}(\tau) &= \tau^{-1} f(\tau), \\ F_0(\tau) &= \tau^{-1} [-1 + \tau^{-1} f(\tau)], & F_1(\tau) &= 2 + 3\tau^{-1} + 3\tau^{-1}(2 - \tau^{-1}) f(\tau), \end{aligned} \quad (24)$$

---

<sup>3</sup>There might exist the contributions from other charged particles such as charginos and heavier stop and sbottoms. The contributions from the charginos are neglected in the present work by assuming them to be heavy while those from the heavier sfermions are neglected because they are very heavy for the parameter set (7).

in terms of the scaling function  $f(\tau)$  [13]:

$$f(\tau) = -\frac{1}{2} \int_0^1 \frac{dy}{y} \ln [1 - 4\tau y(1 - y)] = \begin{cases} \arcsin^2(\sqrt{\tau}), & \tau \leq 1, \\ -\frac{1}{4} \left[ \ln \left( \frac{\sqrt{\tau} + \sqrt{\tau-1}}{\sqrt{\tau} - \sqrt{\tau-1}} \right) - i\pi \right]^2, & \tau \geq 1. \end{cases} \quad (25)$$

It is clear that the imaginary parts of the form factors are developed for the Higgs-boson mass greater than twice the mass of the charged particle running in the loop, i.e.  $\tau \geq 1$  as shown explicitly in Fig. 2. In the presence of weak  $CP$ -violating phases, this development of the imaginary parts can lead to a nonzero polarization asymmetry  $\mathcal{A}_1$ .

## V. NUMERICAL RESULTS

Based on the parameter set (7) for two values of  $\tan \beta = 3, 10$ , we investigate in detail the dependence of the unpolarized part  $\hat{\sigma}_0(H_i)$  and the three polarization asymmetries  $A_i$  for the production of all the three Higgs bosons via two-photon fusion. However, we do not present the cross sections folded with the photon luminosity spectra explicitly because they can be obtained in a rather straightforward way from the partonic cross sections. We do not take into account the QCD radiative corrections either, but for the details we refer to Ref. [14].

Fig. 3 shows the unpolarized cross section  $\hat{\sigma}_0(H_i)$  in units of fb as a function of each Higgs-boson mass  $M_{H_i}$  for five different values of the  $CP$ -violating phase;  $\Phi = 0^\circ$  (thick solid line),  $40^\circ$  (solid line),  $80^\circ$  (dashed line),  $120^\circ$  (dotted line), and  $160^\circ$  (dash-dotted line) by taking  $\tan \beta = 3$  (left column) and  $\tan \beta = 10$  (right column), respectively. We note that for  $\tan \beta = 3$  the phase  $\Phi = 160^\circ$  is not allowed because it violates the bound  $\Delta_f \leq M_{\text{SUSY}}^2$  required to ensure the validity of the loop corrections to the Higgs potential [15,2]. The charged Higgs-boson contributions to the production cross sections are negligible for every Higgs boson because the charged Higgs-boson-pair threshold is much higher than  $M_{H_1}$  and nearly twice as large as the heavier Higgs-boson masses  $M_{H_{2,3}}$  for both  $\tan \beta = 3$  and  $\tan \beta = 10$ .

Firstly, we consider the production of the lightest Higgs boson  $H_1$  with its mass  $m_{H_1}$  less than 130 GeV. For  $\tan \beta = 3$  the cross section  $\hat{\sigma}_0(H_1)$  is dominated by the  $W$  loop contributions which are hardly dependent on the phase  $\Phi$ . On the other hand, for  $\tan \beta = 10$  the  $W$  loop contributions become very sensitive to the  $CP$ -violating phase  $\Phi$  and so does the cross section, especially for a small Higgs-boson mass. Numerically, the first frame of the right column in Fig. 3 shows that the decrease of the cross section with increasing  $\Phi$  is much more significant for a smaller Higgs boson mass.

Secondly, we consider the production of the heavier Higgs bosons  $H_2$  and  $H_3$ . In the case of  $\tan \beta = 3$ , we note:

- In the  $CP$ -invariant theories, i.e. when  $\Phi = 0^\circ$ , the partonic cross section  $\hat{\sigma}_0(H_2)$  has the contributions only from the top-quark loop<sup>4</sup>. This is evident by noting that the

---

<sup>4</sup>Certainly there exists the the bottom-quark loop contribution. However, it is negligible because of its very small Yukawa coupling for  $\tan \beta = 3$ .

thick solid line has a single peak at the top–quark–pair threshold.

- As the phase  $\Phi$  increases, the contributions of the  $W$  boson and light stop loops become sizable; the former contributions are evident for smaller values of  $M_{H_2}$  and the latter ones for larger values of  $M_{H_2}$ . This is because the Higgs boson  $H_2$  develops its  $CP$ –even component with non–trivial  $\Phi$ . The stop contributions always increase the cross section  $\hat{\sigma}_0(H_2)$  above the top–quark–pair threshold. It is noted that there exist small changes below the top–quark–pair threshold due to the new  $W$  loop contributions.
- In the  $CP$ –invariant case the heaviest Higgs boson  $H_3$  is  $CP$ –even so that the main contributions to the cross section  $\hat{\sigma}_0(H_3)$  are from the top–quark loop with the function  $F_{sf}(\tau)$  smoother than the other functions around the top–quark–pair threshold. The steep rise of the cross section with decreasing  $M_{H_3}$  is due to the  $W$  loop contribution near the  $W$ –pair threshold. Near the lighter stop–pair threshold one can see a small bump due to the lighter stop loop contribution.
- The cross section  $\hat{\sigma}_0(H_3)$  increases significantly with the phase  $\Phi$  due to the lighter stop–loop contributions except for smaller values of  $M_{H_3}$ .

In the case of  $\tan\beta = 10$ , we may draw the similar arguments as in the case of  $\tan\beta = 3$  except for two significantly different aspects; (i) the bottom as well as sbottom loop contributions become significant. For example, the small increase of the lower end tail of the thick solid line in the second figure of the right column for  $\Phi = 0^\circ$  is caused by the bottom–quark–loop contribution; (ii) the mass ordering of the heavy  $CP$ –odd and  $CP$ –even Higgs states is completely interchanged for large  $\Phi$ , that is to say,  $H_2$  becomes  $CP$ –even and  $H_3$  becomes  $CP$ –odd for large  $\Phi$ . (This aspect can be seen more clearly by the polarization asymmetry  $\mathcal{A}_3$  for  $\tan\beta = 10$  as will be shown in the following.) This (almost) complete interchange of the  $CP$  properties is reflected in the similar patterns between  $\hat{\sigma}_0(H_2, \Phi = 0^\circ)$  and  $\hat{\sigma}_0(H_3, \Phi = 160^\circ)$  as well as between  $\hat{\sigma}_0(H_2, \Phi = 160^\circ)$  and  $\hat{\sigma}_0(H_3, \Phi = 0^\circ)$  as can be checked in Fig. 3.

The cross sections are not genuine  $CP$ –odd observables so that they cannot allow us to measure the  $CP$ –violating phase directly. On the contrary, as mentioned before, the measurements of the polarization asymmetries enable us to probe  $CP$  violation directly. In order to discuss the polarization asymmetries more efficiently, we first consider the case of  $\tan\beta = 3$ . Fig. 4 shows the polarization asymmetries  $A_i$  as a function of each Higgs–boson mass for four values of the  $CP$ –violating phase;  $\Phi = 0^\circ$  (thick solid line),  $40^\circ$  (solid line),  $80^\circ$  (dashed line), and  $120^\circ$  (dotted line). The left column is for the polarization asymmetry  $\mathcal{A}_1$ , the middle column for the polarization asymmetry  $\mathcal{A}_2$ , and the right column for the polarization asymmetry  $\mathcal{A}_3$ . The polarization asymmetries for the  $CP$ –violating phase  $\Phi$  larger than  $180^\circ$  can be read by the relations

$$\mathcal{A}_{1,2}(\Phi) = -\mathcal{A}_{1,2}(360^\circ - \Phi), \quad \mathcal{A}_3(\Phi) = +\mathcal{A}_3(360^\circ - \Phi), \quad (26)$$

reflecting the fact that the asymmetries  $\mathcal{A}_{1,2}$  are  $CP$ –odd observables and the asymmetry  $\mathcal{A}_3$  a  $CP$ –even observable. We note from Fig. 4 that (i) for the lightest Higgs boson  $H_1$  the asymmetry  $\mathcal{A}_1$  is smaller than 1% and the deviation of the asymmetry  $\mathcal{A}_3$  from the unity is negligible, whereas the asymmetry  $\mathcal{A}_2$  can be as large as 5% if the Higgs boson is light, (ii)

for the heavier Higgs bosons  $H_2$  and  $H_3$ , the asymmetries  $\mathcal{A}_i$  are determined mainly by the top and stop loop contributions above the top–pair threshold, while they are determined by the top and  $W$  loop contributions below the top–pair threshold, and (iii) there exists an additional small contribution from the bottom loop contribution to the asymmetry  $\mathcal{A}_1$  below the  $W$ –pair threshold.

The same polarization asymmetries are displayed as a function of each Higgs-boson mass for the same set of the phases in Fig. 5 by taking a larger value of  $\tan\beta = 10$  rather than  $\tan\beta = 3$  as in Fig. 4. Unlike the small  $\tan\beta$  case,  $\Phi = 160^\circ$  is allowed so that the polarization asymmetries (dash–dotted line) for the phase value are also considered in the discussion. We note from Fig. 5 that (i) even for the lightest Higgs boson  $H_1$ , the polarization asymmetries  $\mathcal{A}_1$  and  $\mathcal{A}_2$  can be as large as 40% and 7%, respectively and the deviation of  $\mathcal{A}_3$  from the unity can be as large as 10% unlike the small  $\tan\beta$  case, (ii) the polarization asymmetries  $\mathcal{A}_i$  for the heavier Higgs bosons  $H_2$  and  $H_3$  are determined mainly by the top/bottom and stop/sbottom loop contributions above the top-quark–pair threshold, while below the top-quark–pair threshold the main contributions come from the top/bottom and  $W$  loops, and (iii) for large  $\Phi$  values ( $\Phi = 120^\circ$  and  $160^\circ$ ) the  $CP$ –parities of the heavier Higgs bosons are interchanged as can be checked in the two lower frames of the right column for  $\mathcal{A}_3$ .

Combining the numerical results from Figs. 4 and 5, we can conclude that for a small  $\tan\beta$  the best  $CP$  observable is the polarization asymmetry  $\mathcal{A}_2$  whereas for a large  $\tan\beta$  the polarization asymmetry  $\mathcal{A}_1$  is the most powerful observable for detecting  $CP$ –violation in the production of the lightest Higgs boson. Therefore, for a small  $\tan\beta$  it is necessary to prepare the colliding photon beams with large linear polarizations, but those with large circular polarizations for a large  $\tan\beta$ . On the other hand, all the polarization asymmetries  $\mathcal{A}_i$  for the heavy Higgs bosons  $H_2$  and  $H_3$  are mostly very sensitive to the the  $CP$ –violating phase  $\Phi$  irrespective of the value of  $\tan\beta$ . Moreover, the polarization asymmetries  $\mathcal{A}_1$  and  $\mathcal{A}_2$  are complementary in the sense that in the mass range where one asymmetry is insensitive to  $\Phi$  the other one is always sensitive to the phase.

## VI. CONCLUSION

We have studied the possibility of measuring the  $CP$  properties of the Higgs bosons in the MSSM with explicit  $CP$  violation in the production of all the three neutral Higgs bosons in two–photon fusion with polarized back–scattered laser photons.

Our detailed analysis has clearly shown that collisions of polarized photons can provide a significant opportunity for detecting  $CP$  violation in the MSSM Higgs sector induced at the loop level from the stop and sbottom sectors.

## ACKNOWLEDGMENTS

The work of SYC was supported by the Korea Science and Engineering Foundation (KOSEF) through the KOSEF–DFG large collaboration project, Project No. 96–0702–01–01–2.

## REFERENCES

- [1] D.A. Demir, Phys. Rev. D **60**, 095007 (1999); S.Y. Choi, hep-ph/9908397.
- [2] A. Pilaftsis and C.E.M. Wagner, Nucl. Phys. **B553**, 3 (1999); D.A. Demir, Phys. Rev. D **60**, 055006 (1999); B. Grzadkowski, J.F. Gunion and J. Kalinowski, hep-ph/9902308.
- [3] T. Ibrahim and P. Nath, Phys. Lett. B **418**, 98 (1998); Phys. Rev. D **57**, 478 (1998); D **58**, 019901 (1998) (E); *ibid.* 111301 (1998); W. Hollik, J.I. Illana, S. Rigolin, C. Schappacher, and D. Stockinger, Nucl. Phys. **B439**, 3 (1999); T. Falk and K.A. Olive, Phys. Lett. B **439**, 71 (1998); M. Brhlik, G.J. Good and G.L. Kane, *ibid.* D **59**, 115004-1 (1999); S. Pokorski, J. Rosiek and C.A. Savoy, hep-ph/9906206; A. Bartl, T. Gajdosik, W. Porod, P. Stochinger and H. Stremnitzer, hep-ph/9903402; E. Accomando, R. Arnowitt, and B. Dutta, hep-ph/9907446; T. Ibrahim and P. Nath, hep-ph/9907555.
- [4] S. Dimopoulos and G.F. Giudice, Phys. Lett. B **357**, 573 (1995); A. Cohen, D.B. Kaplan and A.E. Nelson, *ibid.* B **388**, 599 (1996); A. Pomarol and D. Tommasini, Nucl. Phys. **B488**, 3 (1996); P. Binétruy and E. Duda, Phys. Lett. B **389**, 503 (1996).
- [5] D.A. Demir, A. Masiero and O. Vives, Phys. Rev. Lett. **82**, 2447 (1999); Y.G. Kim, P. Ko and J.S. Lee, Nucl. Phys. **B544**, 64 (1999); S. Baek and P. Ko, Phys. Rev. Lett. **83**, 488 (1999); hep-ph/9904283; hep-ph/9907572; A. Ali and D. London, hep-ph/9903535; hep-ph/9907243.
- [6] T. Falk, A. Frestl and K. Olive, hep-ph/9908311; T. Ibrahim and P. Nath, hep-ph/9907555; hep-ph/9908443; K. Freese and P. Gondolo, hep-ph/9908390.
- [7] J.F. Gunion, B. Grzadkowski, H.E. Haber and J. Kalinowski, Phys. Rev. Lett. **79**, 982 (1997); B. Grzadkowski, J. Gunion and J. Kalinowski, Phys. Rev. D **60**, 075011-1 (1999); S.Y. Choi, J.S. Shim, H.S. Song, and W.Y. Song, Phys. Lett. **B449**, 207 (1999); S.Y. Choi, H.S. Song, and W.Y. Song, hep-ph/9907474, to appear in Phys. Rev. D; S.Y. Choi, M. Guchait, H.S. Song and W.Y. Song, hep-ph/9904276; S.Y. Choi and J.S. Lee, hep-ph/9907496, to appear in Phys. Rev. D; A. Pilaftsis, Phys. Rev. Lett. **77**, 4996 (1996); Nucl. Phys. **B504**, 61 (1997); S.Y. Choi and M. Drees, Phys. Rev. Lett. **81**, 5509 (1998); S.Y. Choi and J.S. Lee, hep-ph/9909315.
- [8] J.F. Gunion and H.E. Haber, Phys. Rev. D **48**, 5109 (1993); D.L. Borden, D.A. Bauer and D.O. Caldwell, *ibid.* D **48**, 4018 (1993);
- [9] D. Grzadkowski and J.F. Gunion, Phys. Lett. B **294**, 361 (1992).
- [10] M. Krämer, J. Kühn, M.L. Stong and P.M. Zerwas, Z. Phys. C **64**, 21 (1994); G.J. Gounaris and G.P. Tsirigoti, Phys. Rev. D **56**, 3030 (1997); D **58**, 059901 (1998) (E).
- [11] I.F. Ginzburg, G.L. Kotkin, S.L. Panfil, V.G. Serbo, and V.I. Telnov, Nucl. Instr. and Math. **219**, 5 (1984).
- [12] D. Chang, W.-Y. Keung and A. Pilaftsis, Phys. Rev. Lett. **82**, 900 (1999); **83**, 3972 (1999) (E); A. Pilaftsis, hep-ph/9909485 v2; D. Chang, W.-F. Chang, and W.-Y. Keung, hep-ph/9910465.
- [13] See, for example, J.F. Gunion, H.E. Haber, G. Kane and S. Dawson, *The Higgs Hunters Guide* (Addison-Wesley Publishing Company, 1990).
- [14] M. Spira, A. Djouadi, D. Graudenz, and P.M. Zerwas, Nucl. Phys. **B453**, 17 (1995) and references therein.
- [15] S.Y. Choi and J.S. Lee, hep-ph/9910557.

## APPENDIX

In this Appendix, we present all the MSSM interaction Lagrangians needed to calculate the contributions of the fermions, the charged Higgs boson, the charged gauge bosons, and the charged sfermions to the two-photon fusion processes  $\gamma\gamma \rightarrow H_i$  ( $i = 1, 2, 3$ ). They are classified in the following four categories;

### 1. Higgs–fermion–fermion couplings:

$$\mathcal{L}_{H\bar{f}f} = -\frac{gm_f}{2m_W} \bar{f} \left[ \left( \frac{v_f^i}{R_\beta^f} \right) - i \left( \frac{\bar{R}_\beta^f a_f^i}{R_\beta^f} \right) \gamma_5 \right] f H_i, \\ R_\beta^f = \begin{cases} c_\beta & , \\ s_\beta & , \end{cases} \quad \bar{R}_\beta^f = \begin{cases} s_\beta & , \\ c_\beta & , \end{cases} \quad v_f^i = \begin{cases} O_{2,4-i} & , \\ O_{3,4-i} & , \end{cases} \quad a_f^i = \begin{cases} O_{1,4-i} & \text{for } f = (l:d) \\ O_{1,4-i} & \text{for } f = (u) \end{cases}. \quad (\text{A1})$$

The  $CP$ –violating neutral Higgs–boson mixing induces a simultaneous coupling of  $H_i$  ( $i = 1, 2, 3$ ) to  $CP$ –even and  $CP$ –odd fermion bilinears  $\bar{f}f$  and  $\bar{f}i\gamma_5 f$ .

### 2. Higgs– $H^+H^-$ vertices:

$$\mathcal{L}_{HH^+H^-} = v C_i H_i H^+ H^- \quad \text{with} \quad C_i = \sum_{\alpha=1,2,3} O_{\alpha,4-i} c_\alpha \quad (\text{A2})$$

with

$$\begin{aligned} c_1 &= 2s_\beta c_\beta \mathcal{I}(\lambda_5 e^{2i\xi}) - s_\beta^2 \mathcal{I}(\lambda_6 e^{i\xi}) - c_\beta^2 \mathcal{I}(\lambda_7 e^{i\xi}), \\ c_2 &= 2s_\beta^2 c_\beta \lambda_1 + c_\beta^3 \lambda_3 - s_\beta^2 c_\beta \lambda_4 \\ &\quad - 2s_\beta^2 c_\beta \mathcal{R}(\lambda_5 e^{2i\xi}) + s_\beta(s_\beta^2 - 2c_\beta^2) \mathcal{R}(\lambda_6 e^{i\xi}) + s_\beta c_\beta^2 \mathcal{R}(\lambda_7 e^{i\xi}), \\ c_3 &= 2c_\beta^2 s_\beta \lambda_2 + s_\beta^3 \lambda_3 - c_\beta^2 s_\beta \lambda_4 \\ &\quad - 2c_\beta^2 s_\beta \mathcal{R}(\lambda_5 e^{2i\xi}) + c_\beta s_\beta^2 \mathcal{R}(\lambda_6 e^{i\xi}) + c_\beta(c_\beta^2 - 2s_\beta^2) \mathcal{R}(\lambda_7 e^{i\xi}). \end{aligned} \quad (\text{A3})$$

Note that the coupling  $c_1$  vanishes in the  $CP$ –invariant theories where the imaginary parts of the quartic couplings  $\lambda_{5,6,7}$  and the induced phase are zero.

### 3. Higgs–sfermion–sfermion vertices:

$$\mathcal{L}_{H_i \tilde{f}_j \tilde{f}_k} = g_{\tilde{f}_j \tilde{f}_k}^i \tilde{f}_j^* \tilde{f}_k H_i, \\ g_{\tilde{f}_j \tilde{f}_k}^i = \tilde{C}_{\alpha;\beta\gamma}^f O_{\alpha,4-i} (U_f)_{\beta j}^* (U_f)_{\gamma k}, \quad (\text{A4})$$

where the index  $\alpha$  denotes three neutral Higgs–boson fields  $\{a, \phi_1, \phi_2\}$  and  $\{\beta, \gamma\}$  the chiralities  $\{L, R\}$ . The unitary matrix  $U_f$  diagonalizes the usual sfermion mass matrix  $\mathcal{M}_{\tilde{f}}^2$  as  $U_f^\dagger \mathcal{M}_{\tilde{f}}^2 U_f = \text{diag}(m_{\tilde{f}_1}^2, m_{\tilde{f}_2}^2)$  with  $m_{\tilde{f}_1} \leq m_{\tilde{f}_2}$ . For the details of the sfermion mixing and the explicit form of the chiral couplings  $\tilde{C}_{\alpha;\beta\gamma}^f$ , we refer to Ref. [15].

### 4. Higgs– $W$ – $W$ vertices:

$$\mathcal{L}_{HW^+W^-} = gm_W (c_\beta O_{2,4-i} + s_\beta O_{3,4-i}) H_i W_\mu^+ W^{-\mu}. \quad (\text{A5})$$

## FIGURES

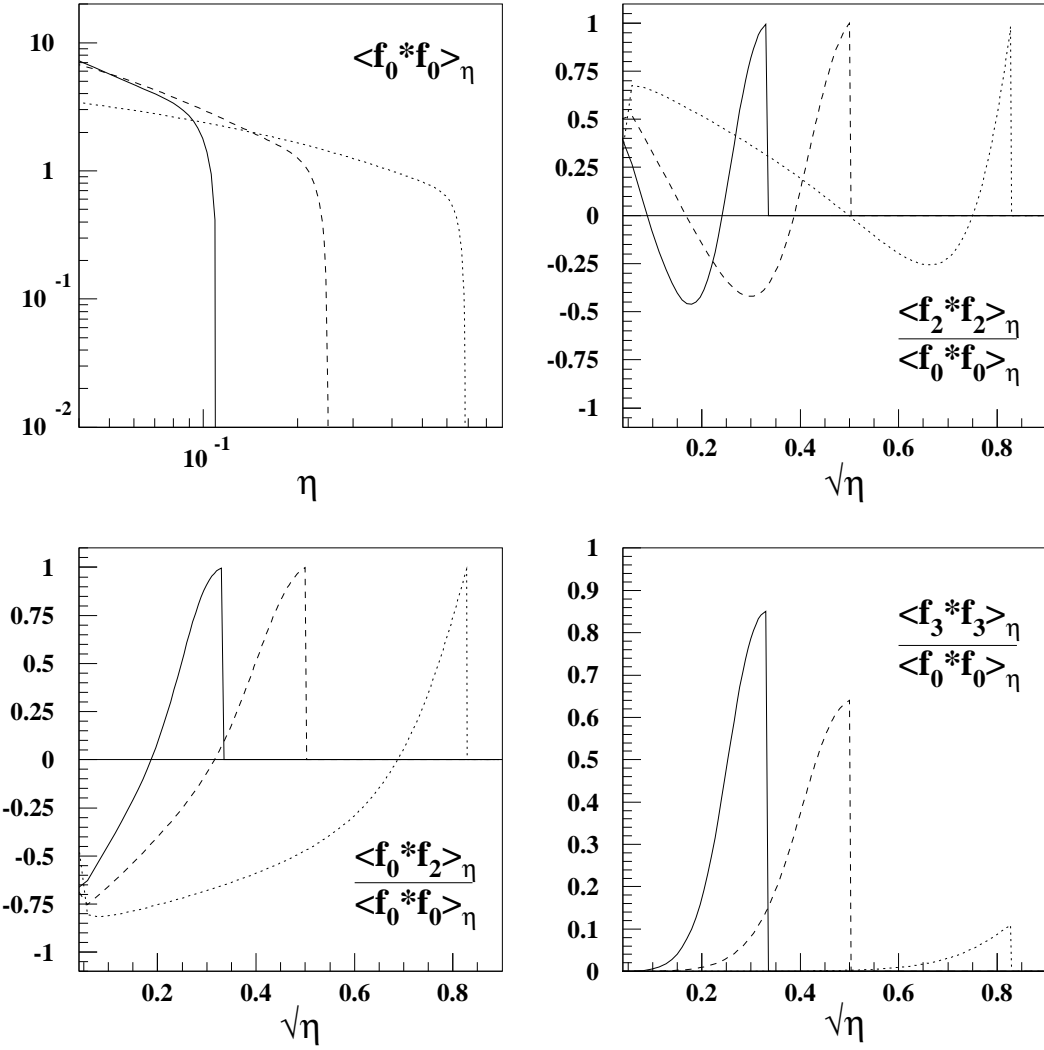


FIG. 1. The luminosity correlation function  $\langle f_0 * f_0 \rangle_\eta$  and the three ratios of the correlation functions for three different values of  $x$ ;  $x = 0.5$  (solid line), 1.0 (dashed line), and 4.83 (dotted line).

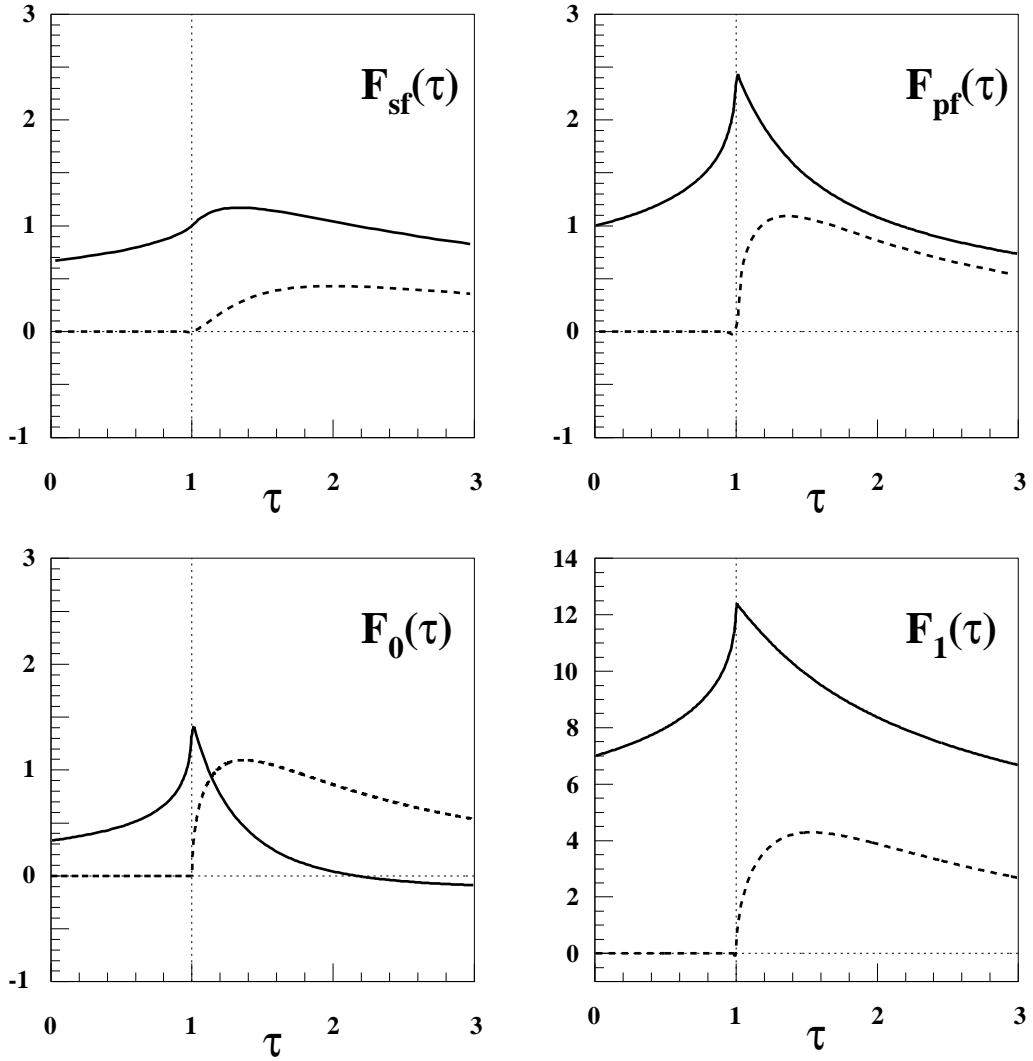


FIG. 2. The real (solid line) and imaginary (dotted line) parts of the form factors  $F_{sf}(\tau)$ ,  $F_{pf}(\tau)$ ,  $F_0(\tau)$  and  $F_1(\tau)$  as a function of the scaling variable  $\tau$ .

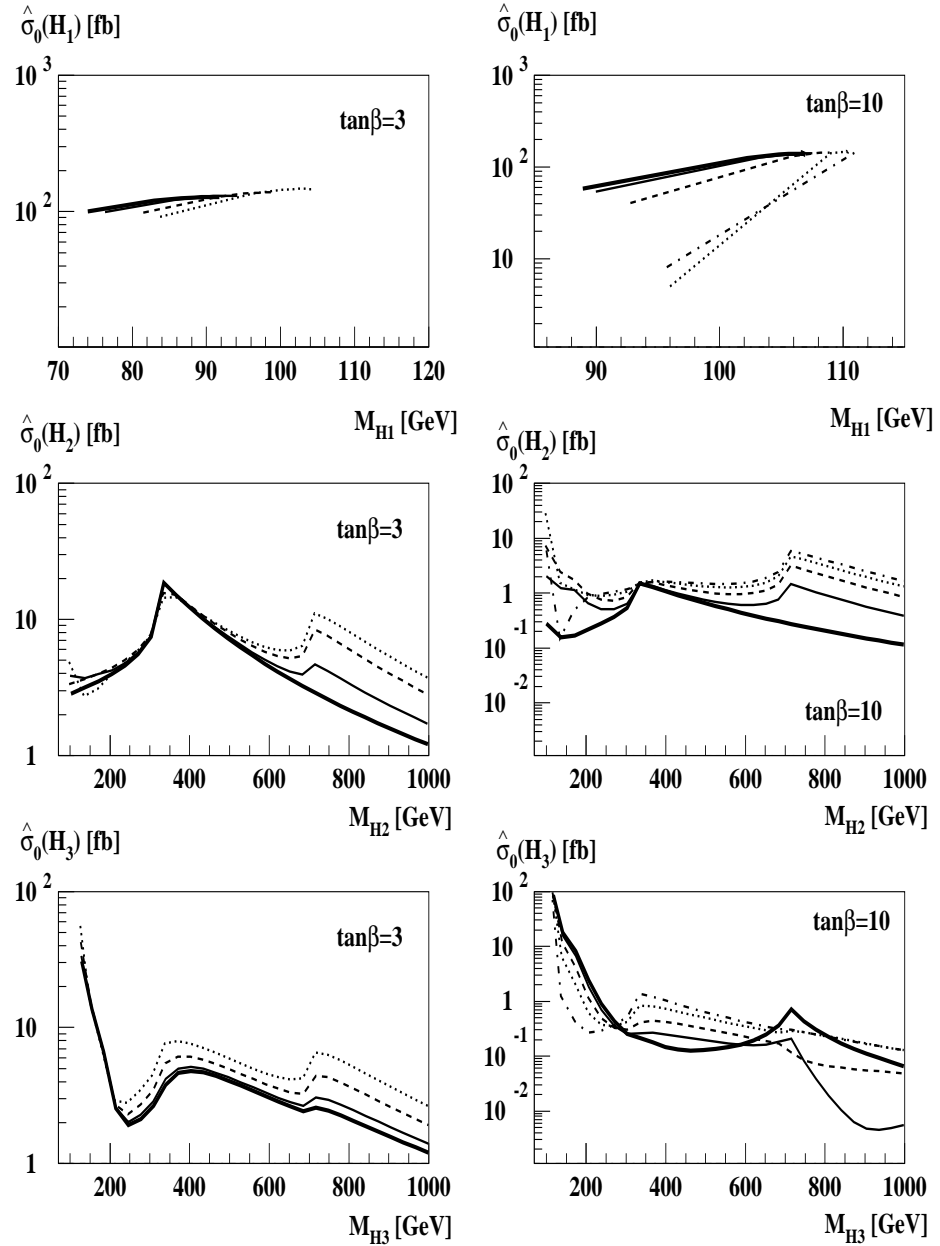


FIG. 3. The partonic cross sections  $\hat{\sigma}_0(H_i)$  in units of fb as a function of each Higgs–boson mass  $M_{H_i}$  ( $i = 1, 2, 3$ ) for five different values of the  $CP$ –violating phase;  $\Phi = 0^\circ$  (thick solid line),  $40^\circ$  (solid line),  $80^\circ$  (dashed line),  $120^\circ$  (dotted line), and  $160^\circ$  (dash–dotted line). The left column is for  $\tan\beta = 3$  and the right column for  $\tan\beta = 10$ .

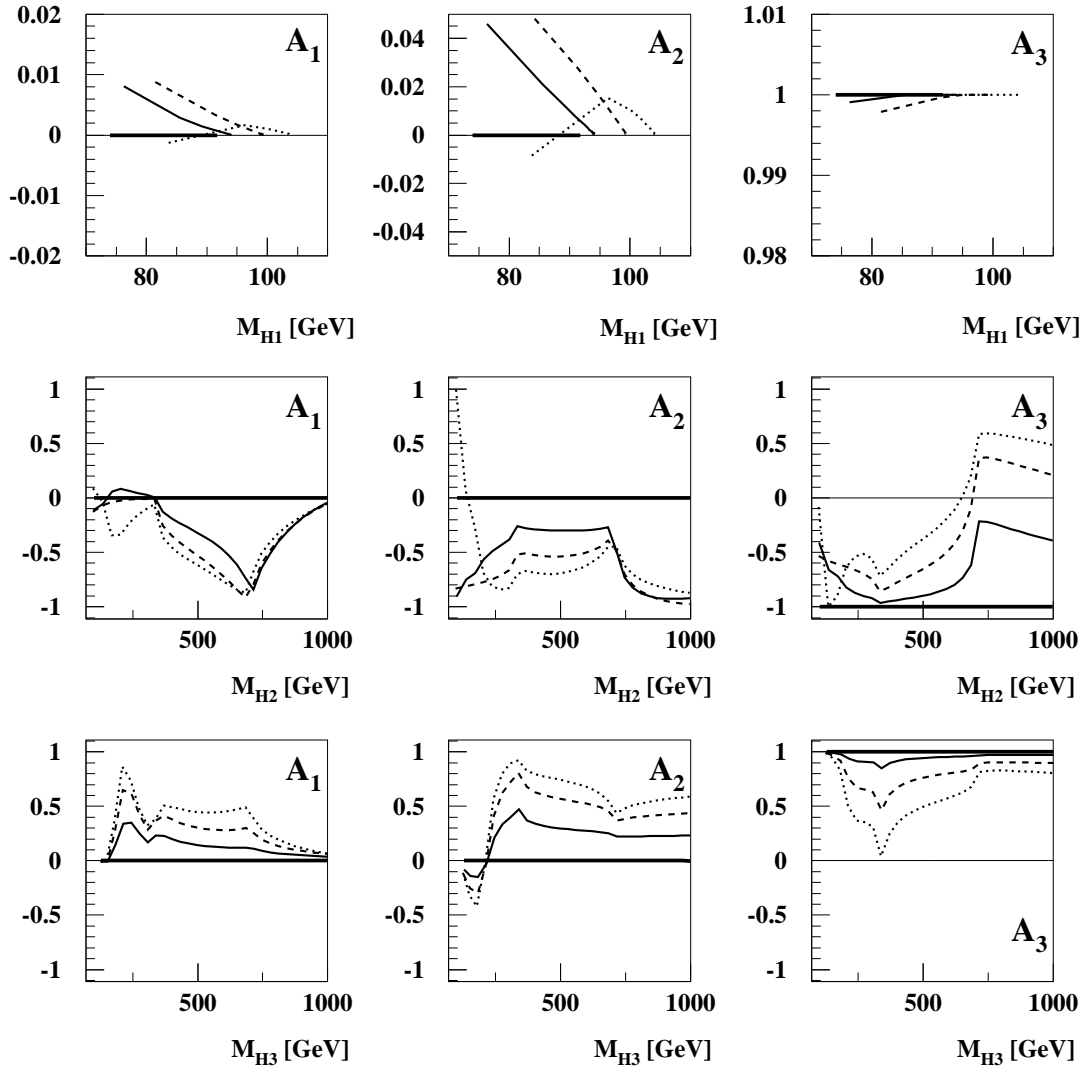


FIG. 4. The polarization asymmetries  $\mathcal{A}_i$  as a function of each Higgs boson mass for four different values of the  $CP$ -violating phase;  $\Phi = 0^\circ$  (thick solid line),  $40^\circ$  (solid line),  $80^\circ$  (dashed line), and  $120^\circ$  (dotted line) in the case of  $\tan\beta = 3$ . The left column is for the asymmetry  $\mathcal{A}_1$ , the middle column for the asymmetry  $\mathcal{A}_2$ , and the right column for the asymmetry  $\mathcal{A}_3$ .

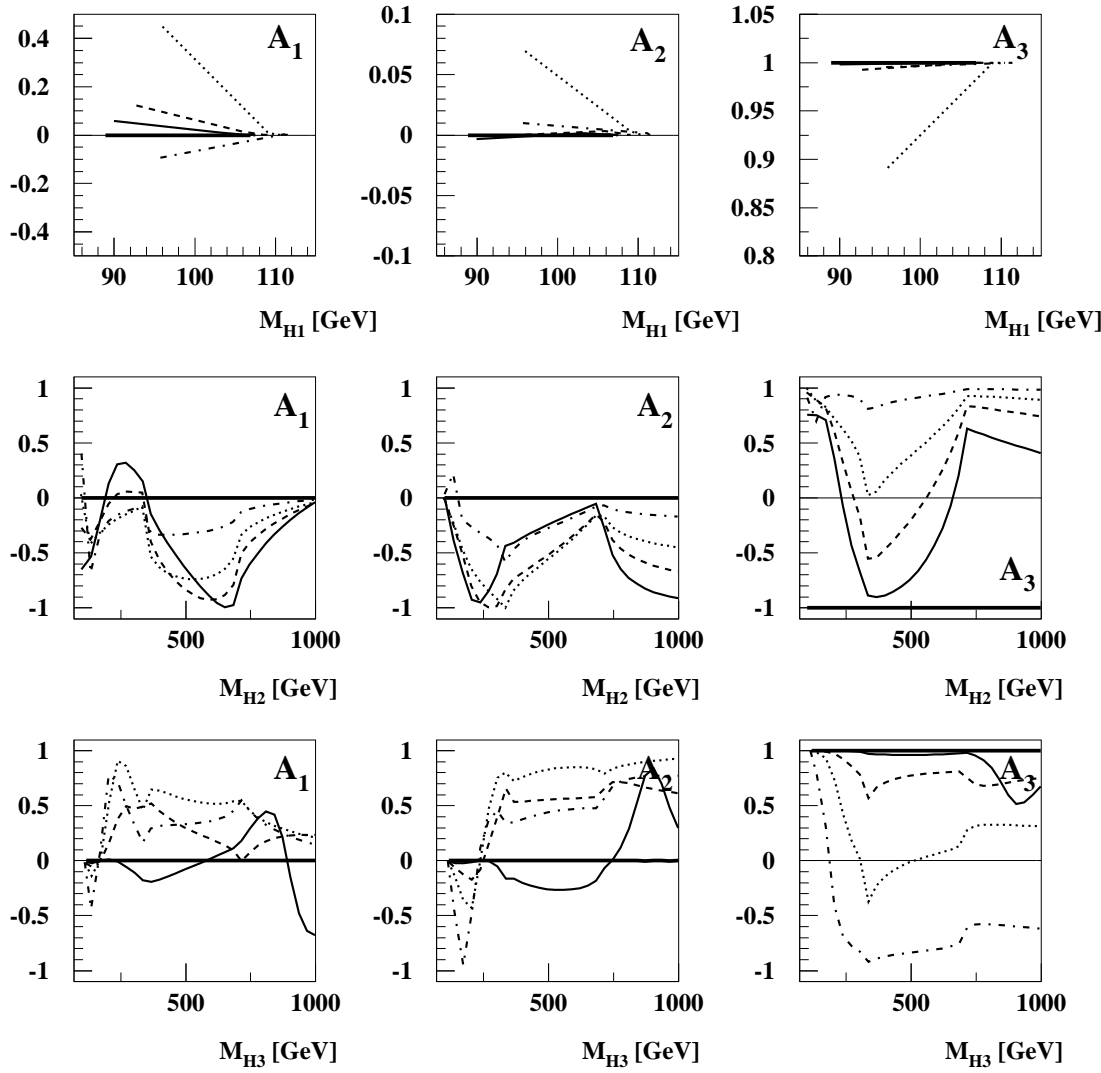


FIG. 5. The polarization asymmetries  $\mathcal{A}_i$  as a function of each Higgs boson mass for five different values of the  $CP$ -violating phase;  $\Phi = 0^\circ$  (thick solid line),  $40^\circ$  (solid line),  $80^\circ$  (dashed line),  $120^\circ$  (dotted line), and  $\Phi = 160^\circ$  (dash-dotted line) in the case of for  $\tan \beta = 10$ . The left column is for the asymmetry  $\mathcal{A}_1$ , the middle column for the asymmetry  $\mathcal{A}_2$ , and the right column for the asymmetry  $\mathcal{A}_3$ .